Laser Physics Letters

LETTER

3D atom microscopy in the presence of Doppler shift

IOP Publishing | Astro Ltd Laser Physics Letters

Laser Phys. Lett. 15 (2018) 035202 (6pp) https://doi.org/10.1088/1612-202X/aa9ac8

Letter

3D atom microscopy in the presence of Doppler shift

Rahmatullah[1,2], You-Lin Chuang[2], Ray-Kuang Lee[2] and Sajid Qamar[1]

[1] Quantum Optics Lab., Department of Physics, COMSATS Institute of Information Technology, Islamabad, Pakistan
[2] Institute of Photonics and Technologies, National Tsing-Hua University, Hsinchu 300, Taiwan

E-mail: sajid_qamar@comsats.edu.pk

Received 23 October 2017, revised 14 November 2017
Accepted for publication 15 November 2017
Published 5 February 2018

Abstract

The interaction of hot atoms with laser fields produces a Doppler shift, which can severely affect the precise spatial measurement of an atom. We suggest an experimentally realizable scheme to address this issue in the three-dimensional position measurement of a single atom in vapors of rubidium atoms. A three-level Λ-type atom–field configuration is considered where a moving atom interacts with three orthogonal standing-wave laser fields and spatial information of the atom in 3D space is obtained via an upper-level population using a weak probe laser field. The atom moves with velocity v along the probe laser field, and due to the Doppler broadening the precision of the spatial information deteriorates significantly. It is found that via a microwave field, precision in the position measurement of a single hot rubidium atom can be attained, overcoming the limitation posed by the Doppler shift.

Keywords: atom microscopy, Doppler shift, standing-wave fields

(Some figures may appear in colour only in the online journal)

Introduction

The quest to achieve precision in position measurement at the atomic scale is not new. However, such measurements are diffraction limited [1] and the spatial resolution achieved is no better than the length scale given by the wavelength of the light field which is used for measurement [2]. In spite of the fundamental nature of the problem, recent advances in laser cooling [3], lithography [4], Bose–Einstein condensates [5] and the measurement of the center-of-mass wave function [6, 7] have made it important to obtain precise position information of the atom. Considerable success has already been attained in the achievement of precision of spatial resolution with near- and far-field imaging techniques [8]. Further, some schemes have been proposed to obtain structures beyond the diffraction limit using position-dependent dark states for nanoscale resolution fluorescence microscopy [9] and in interferometric lithography [10].

Meanwhile, several proposals have been made to obtain position information of moving atoms using quantum optical methods. In these proposals standing-wave driving fields are used to encode the position information into the intensity pattern via the position-dependent Rabi frequency. In the beginning, several schemes were suggested for position measurement of the atom in 1D [11–16]. However, in the last few years, interest has shifted towards 2D atom localization and several schemes have been suggested in this regard [17–20]. It is clear that the next objective would be to achieve 3D atom localization. Some progress has already been made and recently a scheme has been proposed for 3D atom localization in a four-level tripod-type atom–field system using three orthogonal standing-wave fields [21], where eight possible positions of the atom within the cubic optical wavelength in 3D space were noticed. The precision of 3D atom localization can further be enhanced via spatial interference in a two-level atomic system [22] and by three-wave mixing [23]. In a recent

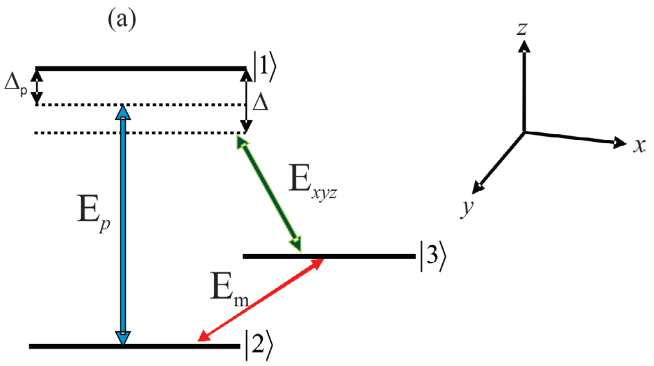

Figure 1. The standing-wave field E_{xyz}, which is the superposition of three orthogonal standing-wave fields that drive the atomic transition $|1\rangle \leftrightarrow |3\rangle$ and a weak probe field E_p that couples the atomic transition $|1\rangle \leftrightarrow |2\rangle$. An additional microwave field E_m is applied corresponding to the transition $|2\rangle \leftrightarrow |3\rangle$.

article, Wang and Yu propose the 3D localization of cold ^{87}Rb atoms with 100% probability via probe absorption in a three-level atomic system [24].

A major limitation of almost all those schemes is that the atom is considered to move through the fields but no Doppler shift is incorporated. In fact, even for a static (cold) atom there is a chance that the atom does not remain perfectly stationary when it is driven by the laser fields. In that case, the motion, which could be modeled as a Gaussian velocity distribution, would affect the precise position measurement of the single atom due to Doppler broadening.

In this article, we examine hot rubidium (^{87}Rb) atoms and propose a scheme for precision enhancement in the position measurement of single atoms in 3D space in the presence of Doppler broadening. Initially, we consider a three-level Λ-type atom–field configuration to obtain precise spatial information of an atom via an upper-level population ignoring the Doppler shift, which is in accordance with earlier work [24]. However, considering a more realistic experimental realization, we incorporate the effect of Doppler broadening, which reduces, significantly, the precision of position measurement of a single atom. To address this problem, we apply an external microwave field corresponding to the atomic transition $|2\rangle \leftrightarrow |3\rangle$. The Λ-type atom–field configuration then becomes a Δ-type configuration and we observe that the Doppler shift is significantly reduced via control of the microwave field. This implies that the precision of position measurement in 3D space can be maintained even in the presence of a Doppler shift.

Theory and discussion

In figure 1, we show the schematic of a three-level atom having one upper level ($|1\rangle$) and two lower levels ($|2\rangle$ and $|3\rangle$). The atom interacts with a standing-wave field E_{xyz}, which is the superposition of three orthogonal standing-wave fields and couples the atomic transition $|1\rangle \leftrightarrow |3\rangle$. To measure the upper-level population, a weak probe laser field E_p is applied which couples the atomic transition $|1\rangle \leftrightarrow |2\rangle$. The resulting atom–field configuration is a Λ-type one, which is experimentally realizable assuming the transition $5S_{1/2} \rightarrow 5P_{3/2}$ in ^{87}Rb. The energy levels can be considered as $|1\rangle = |5P_{3/2}, F=2\rangle$, $|2\rangle = |5S_{1/2}, F=2\rangle$ and $|3\rangle = |5S_{1/2}, F=1\rangle$ [25], which have been used for EIT [26] and for 3D atom localization [24]. An additional microwave field E_m is applied to the atomic transition $|2\rangle \leftrightarrow |3\rangle$, controlling the damaging effects of Doppler broadening. The atom–field configuration thus becomes a Δ-type one (see figure 1). The corresponding Rabi frequencies are $\Omega_p e^{i\phi_p}$, $\Omega_{xyz} e^{i\phi_s}$, and $\Omega_m e^{i\phi_m}$, where ϕ_p, ϕ_s and ϕ_m are the initial phases of the probe, standing-wave and microwave fields. We consider Ω_{xyz} position-dependent.

The standing-wave field E_{xyz} is considered as the superposition of three orthogonal standing-wave fields, i.e. E_x, E_y and E_z, along the x, y and z directions, respectively. We also assume that each standing-wave field is a superposition of the other two standing-wave fields along the corresponding directions. We define the position-dependent Rabi frequency as $\Omega_{xyz} = \Omega_x + \Omega_y + \Omega_z$, with

$$\begin{aligned} \Omega_x &= \Omega_1 \left[\sin(k_1 x + \eta) + \sin(k_2 x)\right], \\ \Omega_y &= \Omega_2 \left[\sin(k_3 y + \varsigma) + \sin(k_4 y)\right], \\ \Omega_z &= \Omega_3 \left[\sin(k_5 z + \varphi) + \sin(k_6 z)\right], \end{aligned} \tag{1}$$

where $k_i = 2\pi/\lambda_i \, (i = 1, 2, 3, 4, 5, 6)$ denotes the wave-vectors having the wavelengths $\lambda_i \, (i = 1, 2, 3, 4, 5, 6)$ of the corresponding standing-wave fields. The parameters η, ς and φ are the phase shifts associated with the standing-wave fields with wave-vectors k_1, k_3 and k_5, respectively.

The interaction picture Hamiltonian for the system in the dipole and rotating-wave approximation can be written as

$$H = -\hbar \left[\Omega_p e^{i\Delta_p t} |1\rangle\langle 2| + \Omega_{xyz} e^{i\Delta t} |1\rangle\langle 3| + \Omega_m e^{i\phi} |3\rangle\langle 2| + H.c\right], \tag{2}$$

where $\Delta_p = \omega_{12} - \nu_p$ and $\Delta = \omega_{13} - \nu$ are the detuning associated with the probe and standing-wave fields corresponding to the atomic transitions $|1\rangle \leftrightarrow |2\rangle$ and $|1\rangle \leftrightarrow |3\rangle$, respectively, and $\phi = \phi_m + \phi_s - \phi_p$ is the relative phase of the standing-wave, probe and microwave fields.

The equations of motion for the corresponding density matrix elements can be written as

$$\begin{aligned} \dot{\rho}_{11} &= -(\Gamma_{12} + \Gamma_{13}) \rho_{11} - i\Omega_p (\rho_{12} - \rho_{21}) - i\Omega_{xyz} (\rho_{13} - \rho_{31}), \\ \dot{\rho}_{22} &= \Gamma_{12}\rho_{11} + \Gamma_{32}\rho_{33} + i\Omega_p (\rho_{12} - \rho_{21}) + i\Omega_m \left(e^{-i\phi}\rho_{32} - e^{i\phi}\rho_{23}\right), \\ \dot{\rho}_{33} &= \Gamma_{13}\rho_{11} - \Gamma_{32}\rho_{33} + i\Omega_{xyz} (\rho_{13} - \rho_{31}) - i\Omega_m \left(e^{i\phi}\rho_{32} - e^{-i\phi}\rho_{23}\right), \\ \dot{\rho}_{23} &= i(\Delta_p - \Delta + i\gamma_{23}) \rho_{23} + i\Omega_p \rho_{13} - i\Omega_{xyz}\rho_{21} - i\Omega_m e^{-i\phi} (\rho_{22} - \rho_{33}), \\ \dot{\rho}_{21} &= i(\Delta_p + i\gamma_{21}) \rho_{21} - i\Omega_p (\rho_{22} - \rho_{11}) - i\Omega_{xyz}\rho_{23} + i\Omega_m e^{-i\phi}\rho_{31}, \\ \dot{\rho}_{31} &= i(\Delta_p + i\gamma_{31}) \rho_{31} - i\Omega_{xyz} (\rho_{33} - \rho_{11}) - i\Omega_p\rho_{32} + i\Omega_m e^{i\phi}\rho_{21}. \end{aligned} \tag{3}$$

Here $\Gamma_{ij} \, (ij \in 1, 2, 3, \; i \neq j)$ is the decay rate from level $|i\rangle$ to level $|j\rangle$, where $\gamma_{23} = \Gamma_{32}/2, \gamma_{21} = (\Gamma_{12} + \Gamma_{13})/2$, and $\gamma_{31} = (\Gamma_{32} + \Gamma_{12} + \Gamma_{13})/2$.

Our objective is to obtain position information of the atom via absorption of the probe field, which is directly related to the upper-level population ρ_{11}. Initially, the atom is considered to be in the ground state $|2\rangle$ and when the probe field is absorbed the atom is excited to the upper-level $|1\rangle$. The probability of an upper-level population can thus be termed the conditional position probability of the atom in 3D space. To understand the dependence of the upper-level population on certain parameters like Ω_p, Ω_{xyz}, Ω_m and Δ_p, we use equation (3) and calculate the analytical expression for the upper-level populations:

$$\rho_{11}(\Delta_p) = \frac{\Omega_p^2(\Delta_p-\Delta)^2}{[((\Delta_p-\Delta)\Delta_p-\Omega_{xyz}^2))^2+\gamma_{21}^2(\Delta_p-\Delta)^2]} - \frac{\Omega_p\Omega_{xyz}\Omega_m e^{i\phi}}{[((\Delta_p-\Delta)\Delta_p-\Omega_{xyz}^2))^2+\gamma_{21}^2(\Delta_p-\Delta)^2]}, \quad (4)$$

with $\Gamma_{32} = 0$ and $\gamma_{21} = \gamma_{31}$.

We consider $\rho_{11}(\Delta_p)$ as the filter function which determines the 3D conditional position probability distribution of the atom. The first term in equation (4) corresponds to the EIT phenomenon while the second term, which involves the microwave field, describes the gain process [27]. The 3D conditional position probability distribution can be controlled via the interference of the two terms. It is well known that for the Λ-type atom–field configuration coherent population trapping occurs for the two-photon resonance condition and the ground-level population never goes to zero [28]. We, however, consider that the two detuning parameters Δ and Δ_p are far detuned from each other. Thus, we avoid the two-photon resonance condition, and as a result we can obtain the maximum population of the excited level $|1\rangle$. For $\Delta = 0$, the probe detuning condition becomes $\Delta_p = 2\Omega(\sin kx + \sin ky + \sin kz)$ when $\xi = \varsigma = \phi = 0$ and $k_i = k$ $(i = 1, 2, 3, 4, 5, 6)$, which may lead to the maxima in the 3D conditional position probability distribution. One can notice that the position probability distribution of the atom in 3D space, which is conditioned upon the measurement of the upper-level population or probe absorption and leads to the 3D spatial measurement of the atom, is directly related to the probe field detuning. However, we are considering a general case and carrying out a numerical analysis of the position measurement of a moving atom, i.e. without considering any approximation on Ω_p or $\Omega_i (i = 1, 2, 3)$.

We first ignore the effect of a Doppler shift and show the best possible spatial measurement of a single atom using a Λ-type atom–field configuration. The parameters we select are $\Omega = 2.3\Gamma$, $\Omega_p = 0.1\Gamma$, $\Omega_m = 0$ $(E_m = 0)$, $\Delta = 0$, $\Delta_p = 13.8\Gamma$, $k_1 = k_3 = k_5 = 0.8\kappa, \eta = \varsigma = \varphi = \pi/8$, $\Gamma_{12} = \Gamma_{13} = 0.5\Gamma$ and $\Gamma_{32} = 0$ $(\Gamma = 6\,\text{MHz})$. In the absence of the microwave field ($\Omega_m = 0$), the second term in equation (4) becomes zero and the 3D conditional position probability distribution of the atom only depends on the EIT phenomenon. The values for the decay rate Γ and Rabi frequencies correspond to [26]. Following the same procedure utilized in [7, 16, 20], we consider slightly different wavelengths and the phase shifts associated with the standing-wave fields. The plot of the filter function $\rho_{11}(\Delta_p)$ versus the normalized positions κx, κy and κz shows a single 3D peak, which is reflected as a sphere in the xyz space (see figure 2(a)). The sphere describes the 3D position probability distribution of the atom and shows the possible position of the atom within a cubic optical wavelength. The size of the surface of the sphere defines the full width at half maximum in 3D space.

To determine where exactly the center of the sphere is located, we show the 2D views of the filter function $\rho_{11}(\Delta_p)$ in figures 2(b)–(d). From these figures, we can observe that the sphere is centered at $\pi/2$, $\pi/2$, $\pi/2$, which determines the position of the atom in the 3D xyz space.

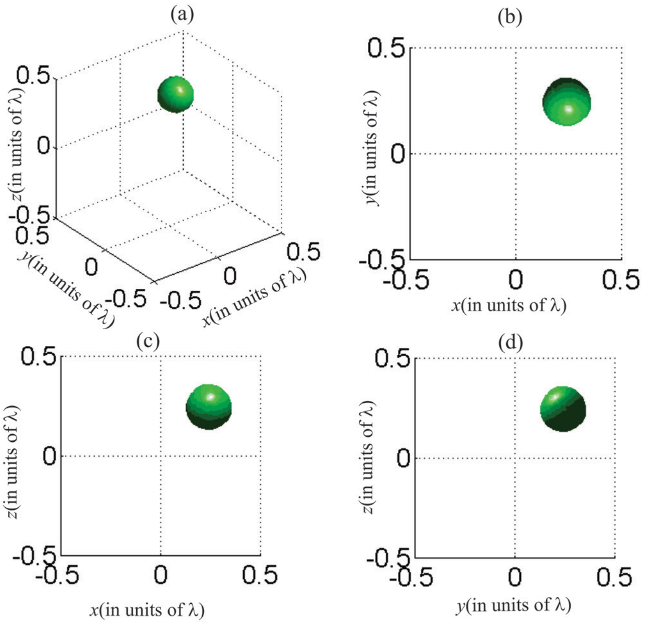

Figure 2. 3D atom localization: (a) upper-level population as a function of κx, κy and κz; (b)–(d) xy, xz, and yz view of (a), respectively. The other parameters are $\Omega = 2.3\Gamma$, $\Omega_p = 0.1\Gamma$, $\Omega_m = 0$, $\Delta = 0$, $\Delta_p = 13.8\Gamma$, $\Gamma_{12} = \Gamma_{13} = 0.5\Gamma$, $k_1 = k_3 = k_5 = 0.8\kappa$, $k_2 = k_4 = k_6 = \kappa$, $\phi = 0$, $\eta = \varsigma = \varphi = \pi/8$, and $\Gamma_{32} = 0$ $(\Gamma = 6\,\text{MHz})$.

Here we would like to emphasize that this is not the only possible position of the atom in the xyz space—one can get other positions as well. For example, by just changing the values of the phase shifts from $\eta = \varsigma = \pi/8$ to $\eta = \varsigma = -\pi/8$, one can obtain a new position of the atom, i.e. $-\pi/2, -\pi/2, -\pi/2$, instead of $\pi/2, \pi/2, \pi/2$ in the xyz space. These results also show that the precision of spatial measurement of a single atom within a cubic wavelength is enhanced by a factor of 8 over that in [21].

Until now, we have not incorporated the effect of the Doppler shift; however, our main objective is to consider that the atom is not stationary during its interaction with the laser fields and consider that the atom moves with velocity v along the direction of the probe field [29]. In this case, the effect of Doppler broadening on the 3D spatial measurement of the atom must be considered. In the following, we consider that the atom moves in the z direction, i.e. perpendicularly to the standing-wave fields acting along the x and y directions. Only the fields in the direction of the motion of the atom are important to accounting for the effect of a Doppler shift. In the present case, only the probe field and one of the standing-wave fields, e.g. E_z, are considered to propagate along the direction of the motion of the atom and we only consider these two fields to investigate the effect of Doppler broadening. As standing-wave field E_z is constructed from two counter-propagating beams, for the resonant interaction between the atom and standing-wave field, there are no shifts in the frequency of the standing-wave field. The reason is that the counter-propagating fields cancel each other's shift. Let us only consider the Doppler shift corresponding to the probe field and replace the probe field detuning Δ_p with $\Delta_p + k_p v$ in equation (3), where k_p is the wave-vector of the probe field and v is the velocity of

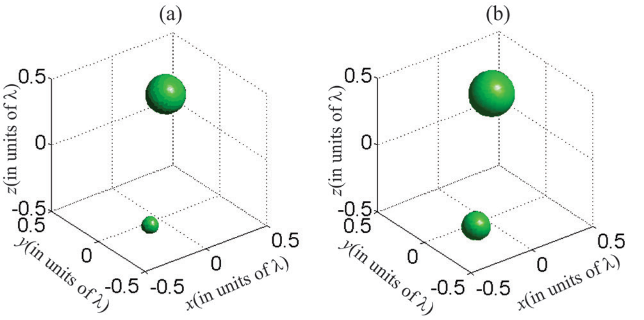

Figure 3. Plot of 3D conditional position probability distribution versus normalized positions κx, κy and κz for different values of Doppler width D: (a) $D = 0.3\Gamma$ and (b) $D = \Gamma$. The remaining parameters are the same as those used in figure 2(a).

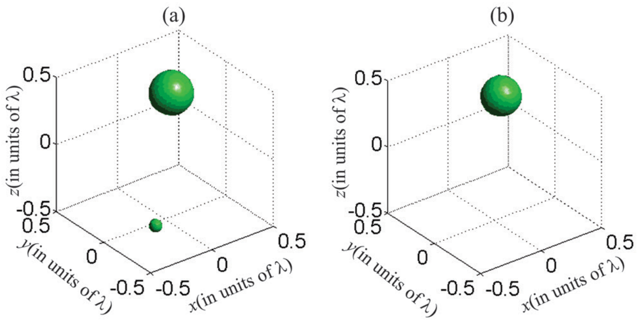

Figure 4. Plot of 3D conditional position probability distribution versus normalized positions κx, κy and κz for different values of magnetic field $\Omega_{\rm m}$: (a) $\Omega_{\rm m} = 0.03\Gamma$ and (b) $\Omega_{\rm m} = 0.04\Gamma$. The remaining parameters are the same as those used in figure 3(b).

the atom. To obtain the upper-level population in a Doppler-broadened medium, velocity-dependent $\rho_{11}(\Delta_{\rm p} + k_{\rm p}v)$ should be integrated over the Maxwell–Boltzmann distribution for the atomic velocities. In the presence of a Doppler effect, the upper-level population can be written as

$$\rho_{11}(d) = \frac{1}{\sqrt{2\pi}D}\int_{-\infty}^{\infty}\rho_{11}\left(\Delta_{\rm p} + k_{\rm p}v\right)\mathrm{e}^{-(v)^2/2D^2}\mathrm{d}(v), \quad (5)$$

where $D = \sqrt{k_{\rm p}^2 K_{\rm B} T/M}$ is the Doppler width. $K_{\rm B}$, T and M are the Boltzmann constant, absolute temperature and mass of the atom, respectively. We call $\rho_{11}(d)$ the Doppler-broadened filter function for the 3D conditional position probability distribution.

In figure 3, we plot the Doppler-broadened 3D filter function versus the normalized positions κx, κy and κz in the xyz space for two different values of the Doppler width, i.e. D equal to (a) 0.3Γ and (b) Γ, while keeping the other parameters the same as in figure 2(a). The precision of the position of the atom reduces as we introduce the Doppler effect and a second sphere starts appearing. The size of the second sphere, which was not present in the absence of Doppler broadening, increases as we increase the value of the Doppler width (see figures 3(a) and (b)). This shows that the precision of position measurement of a single atom reduces significantly in the presence of the Doppler shift. This implies that for a better spatial measurement of the atom with the best possible spatial resolution, one needs to have a Doppler-free spectroscopy, which seems impossible unless one has ultra-cold atoms. Another possibility one can think of is to eliminate the Doppler shift if the probe field is acting along the x or y direction perpendicularly to the motion of the atom or if one must consider that the motion of the atom is classical. The former, i.e. using ultra-cold atoms, limits practical applications, e.g. in atom lithography at room temperature. The latter is a more approximate solution and does not mimic the real scenario. In the following, we address this issue and discuss that in the presence of a microwave field, the effect of the Doppler shift can be reduced and the precision of spatial measurement of a single atom can be attained even in the presence of Doppler broadening.

We apply a microwave field $E_{\rm m}$, which drives the atomic transition $|2\rangle \leftrightarrow |3\rangle$. In the presence of this field, the coherence of the two ground states is perturbed, which affects the transmission of the probe light. The resulting quantum interference can lead to suppression or enhancement of EIT depending on the relative phase between the optical and microwave fields [30]. Here, we consider zero relative phase in which one of the EIT peaks is suppressed [27]. This suppression of the EIT peak occurs even in the presence of a Doppler shift [31]. Therefore, in the proposed model for atom microscopy, one of the spheres can vanish according to the suppression of EIT. This is evident from equation (4): when the microwave field is turned on, the second term starts playing its role. As a result, the 3D conditional position probability distribution now depends on the interference between the two terms in equation (4). Here, we consider a static magnetic field to ignore degeneracy [32]. We now plot the Doppler-broadened 3D filter function $\rho_{11}(d)$ versus the normalized positions κx, κy and κz for two Rabi frequencies $\Omega_{\rm m}$, i.e. (a) 0.03Γ and (b) 0.04Γ, corresponding to the microwave field $E_{\rm m}$. We notice that one of the two spheres in figure 3 starts diminishing and precision in position measurement of the moving atom can be attained even in the presence of a Doppler shift (see figure 4).

In our proposed atom–field system, the applied fields acting on the atom form a closed loop, resulting in a Δ-type configuration. As a result, the optical properties of the system strongly depend on the relative phase φ of the applied fields. Therefore, in the following we consider the role of φ in the precise position measurement of a moving atom in the presence of Doppler broadening.

It is clear that there are two paths to exciting the atom to the upper level $|1\rangle$: one is by making a direct transition from the ground energy level $|2\rangle$ to the excited level $|1\rangle$ and another is indirect transition from $|2\rangle$ to $|1\rangle$ via the intermediate level $|3\rangle$. These two atomic transition paths interfere with each other either constructively or destructively depending on the choice of relative phase φ. In figure 4, for $\varphi = 0$, we notice that precision enhancement of 3D position information is achieved via control of the microwave field even in the presence of Doppler broadening. However, as can be observed from equations (3)–(5), the 3D conditional position probability distribution is sensitive to the relative phase ϕ. In figure 5, we plot the 3D conditional position probability distribution for four different non-zero values of the relative phase ϕ, i.e. (a) $\phi = \pi/8$, (b)

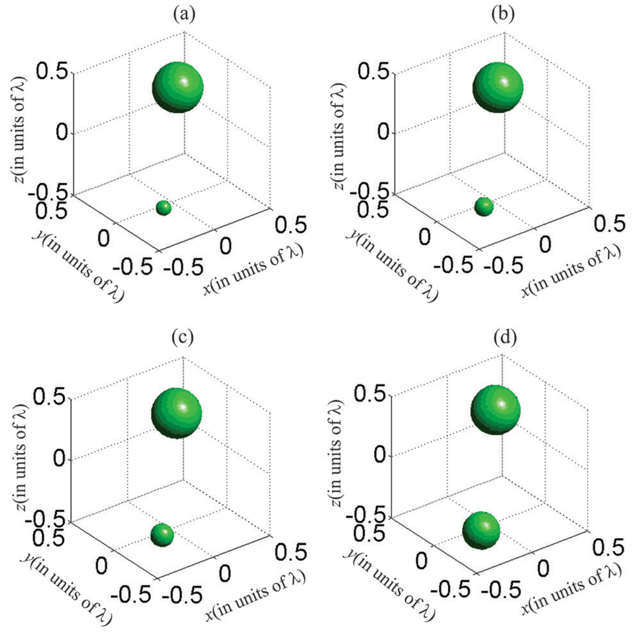

Figure 5. Plot of 3D conditional position probability distribution versus normalized positions κx, κy and κz for different values of relative phase ϕ: (a) $\phi = \pi/8$, (b) $\phi = \pi/6$, (c) $\phi = \pi/4$ and (d) $\phi = \pi/2$. The remaining parameters are the same as those used in figure 4(b).

$\phi = \pi/6$, (c) $\phi = \pi/4$ and (d) $\phi = \pi/2$. It can be observed that the precision of 3D position information reduces as the relative phase becomes $\phi = \pi/2$.

Conclusion

We have considered an experimentally realizable scheme based on a Δ-type atom–field configuration [30] for the precise position measurement of hot ^{87}Rb atoms. Our scheme is a possible solution to overcome the issues in the precise position measurement of atoms, which is influenced by the Doppler shift. The position of a single atom which is Doppler shifted in 3D space can be obtained with high precision via control of an external microwave field with a relative phase equal to zero, i.e. $\varphi = 0$.

Acknowledgments

Rahmatullah would like to thank Ziauddin for valuable discussions and the Ministry of Science and Technology, Taiwan, for its support and travel grant.

References

[1] Born M and Wolf E 1999 *Principles of Optics* (Cambridge: Cambridge University Press)
[2] Heisenberg W 1927 *Z. Phys.* **43** 172
[3] Phillips W D 1998 *Rev. Mod. Phys.* **70** 721
[4] Johnson K S, Thywissen J H, Dekker N H, Berggren K K, Chu A P, Younkin R and Prentiss M 1998 *Science* **280** 1583
[5] Collins G P 1996 *Phys. Today* **49** 18
[6] Kapale K T, Qamar S and Zubairy M S 2003 *Phys. Rev.* A **67** 023805
[7] Evers J, Qamar S and Zubairy M S 2007 *Phys. Rev.* A **75** 053809
[8] Lewis A, Isaacson M, Harootunian A and Muray A 1984 *Ultramicroscopy* **13** 227
Lewis A, Taha H, Strinkovski A, Manevitch A, Khatchatourians A, Dekhter R and Ammann E 2003 *Nat. Biotechnol.* **21** 1378
Hell S and Stelzer E H K 1992 *J. Opt. Soc. Am.* A **9** 2159
Hell S W and Wichmann J 1994 *J. Opt. Lett.* **19** 780
Klar T A, Jakobs S, Dyba M, Egner A and Hell S W 2000 *Proc. Natl Acad. Sci. USA* **97** 8206
[9] Bretschneider S, Eggeling C and Hell S W 2007 *Phys. Rev. Lett.* **98** 218103
Yavuz D D and Proite N A 2007 *Phys. Rev.* A **76** 041802
Gorshkov A V, Jiang L, Greiner M, Zoller P and Lukin M D 2008 *Phys. Rev. Lett.* **100** 093005
[10] Kiffner M, Evers J and Zubairy M S 2008 *Phys. Rev. Lett.* **100** 073602
Li H, Sautenkov V A, Kash M M, Sokolov A V, Welch G R, Rostovtsev Y V, Zubairy M S and Scully M O 2008 *Phys. Rev.* A **78** 013803
[11] Herkommer A M, Schleich W P and Zubairy M S 1997 *J. Mod. Opt.* **44** 2507
Qamar S, Zhu S Y and Zubairy M S 2000 *Opt. Commun.* **176** 409
Qamar S, Zhu S Y and Zubairy M S 2000 *Phys. Rev.* A **61** 063806
[12] Paspalakis E and Knight P L 2001 *Phys. Rev.* A **63** 065802
Paspalakis E, Terzis A F and Knight P L 2005 *J. Mod. Opt.* **52** 1685
[13] Ghafoor F, Qamar S and Zubairy M S 2002 *Phys. Rev.* A **65** 043819
[14] Sahrai M, Tajalli H, Kapale K T and Zubairy M S 2005 *Phys. Rev.* A **72** 013820
Kapale K T and Zubairy M S 2006 *Phys. Rev.* A **73** 023813
[15] Agarwal G S and Kapale K T 2006 *J. Phys. B: At. Mol. Opt. Phys.* **39** 3437
[16] Qamar S, Evers J and Zubairy M S 2009 *Phys. Rev.* A **79** 043814
Qamar S, Mehmood A and Qamar S 2009 *Phys. Rev.* A **79** 033848
Asghar S and Qamar S 2013 *Opt. Commun.* **295** 145
[17] Ivanov V and Rozhdestvensky Y 2010 *Phys. Rev.* A **81** 033809
[18] Ding C, Li J, Zhan Z and Yang X 2011 *Phys. Rev.* A **83** 063834
Ding C, Li J, Yu R, Hao X and Wu Y 2012 *Opt. Express* **20** 7870
Ding C, Li J, Yang X, Zhang D and Xiong H 2011 *Phys. Rev.* A **84** 043840
[19] Wan R G, Kou J, Jiang L, Jiang Y and Gao J Y 2011 *J. Opt. Soc. Am.* B **28** 10
Wan R G, Kou J, Jiang L, Jiang Y and Gao J Y 2011 *J. Opt. Soc. Am.* B **28** 622
Wan R G and Zhang T Y 2011 *Opt. Express* **19** 25823
Wan R G, Zhang T Y and Kou J 2013 *Phys. Rev.* A **87** 043816
[20] Rahmatullah and Qamar S 2013 *Phys. Rev.* A **88** 013846
Rahmatullah and Qamar S 2013 *Phys. Lett.* A **378** 684
Rahmatullah, Wahab A and Qamar S 2014 *Laser Phys. Lett.* **11** 045202
[21] Ivanov V, Rozhdestvensky Y and Suominen K 2014 *Phys. Rev.* A **90** 063802
[22] Zhu Z H *et al* 2016 *Phys. Rev.* A **94** 013826
[23] Zhu Z H, Chen A X, Liu S P and Yang W X 2016 *Phys. Lett.* A **380** 3956
[24] Wang Z and Yu B 2015 *J. Opt. Soc. Am.* B **32** 1281
[25] Steck D A 2015 Rubidium 87 D line data (available at http://steck.us/alkalidata)

[26] Wang J, Zhu Y, Jiang K J and Zhan M S 2003 *Phys. Rev.* A **68** 063810

[27] Joo J, Bourassa J, Blais A and Sanders B C 2010 *Phys. Rev. Lett.* **105** 073601

[28] Gray H R, Whitley R M and Stroud C R 1978 *Opt. Lett.* **3** 218

[29] Yan H, Liao K Y, Li J F, Du Y X, Zhang Z M and Zhu S L 2013 *Phys. Rev.* A **87** 055401

[30] Li H, Sautenkov V A, Rostovtsev Y V, Welch G R, Hammer P H and Scully M O 2009 *Phys. Rev.* A **80** 023820

[31] Manjappa M, Undurti S S, Karigowda A, Narayanan A and Sanders B C 2014 *Phys. Rev.* A **90** 043859

[32] Wei X G, Wu J H, Sun G X, Shao Z, Kang Z H, Jiang Y and Gao J Y 2005 *Phys. Rev.* A **72** 023806